Radiation Thermometry (December 2014)

Daphne Chou, Jon Heiselman, Sixian Hong, Laura Slykhouse, University of Michigan - Ann Arbor

***Abstract*—There is a need for non-invasive, non-contact monitoring of core body temperature in situations such as surgery. Current methods of IR thermometry require a user to continuously hold the thermometer in the ear. In this paper, we describe the design of a non-invasive radiation thermometer and subsequent calibration of the sensor to monitor core body temperature using measurements at the ear and at other parts of the body.**

***Index Terms*—Radiation, Infrared, Thermometry**

I. Introduction

Maintaining body temperature homeostasis is crucial for normal functioning. A healthy, normal temperature is considered to be around 37 degrees Celsius. A core body temperature above this level can result in hyperthermia, while a core body temperature below this level can result in hypothermia. Extreme temperature fluctuations can result in permanent disability or even death. Therefore, there is an acute need for accurate monitoring of core temperature. This method of temperature detection should be non-invasive and fast to allow for continuous and convenient monitoring of core body temperature. Knowing that objects emit radiation proportional to their temperature, IR radiation thermometers measure the radiation emitted from an object to determine its temperature.

The objective was to design and build a radiation thermometer using temperature-sensitive sensors and output voltages proportional to radiation intensity. Next, the signals were inputted to a LabVIEW VI that calibrated the thermometer system. This calibration step determined constants that related temperature readings at the ear and neck to core body temperature. The last step of calibration allowed users to input established calibration constants for monitoring of patient core body temperature.

II. Experimental Set-up

Our designed system could be divided into three different parts: the sensor part, the conditioning circuit part, and the LabVIEW part.

A. Sensor Hardware

A TPS 333 thermopile detector was used to transduce IR radiation intensity to a measurable voltage. The TPS 333 also included a thermistor in its housing to supply a measure of ambient temperature. A sheet of aluminum foil taped to a sheet of paper for rigidity was made into a tube and affixed to the end of the sensor. The foil tube reflected IR radiation through with minimal loss while distancing the sensor from warming heat sources in order to prevent temperature drift of the thermistor. An IR LED and phototransistor were attached to the sensor alongside one another and shielded to measure the distance between the tip of the sensor and the target. Three-foot long leads from each component of our mobile sensor were then given to the conditioning circuit.

B. Conditioning Circuit

We used an AD620 instrumentation amplifier to capture the small voltage difference outputted by the thermopile while amplifying the signal by 2200 times to produce a signal suitable for acquisition by the DAQ board. This signal was then filtered with a low-pass cutoff of $10Hz$ and unity gain to remove high frequency noise picked up by the long leads to our sensor. This cutoff was chosen according to the TPS 333 specification sheet that displays the amplitude of the thermopile signal sharply diminishing past a frequency of $10Hz$.

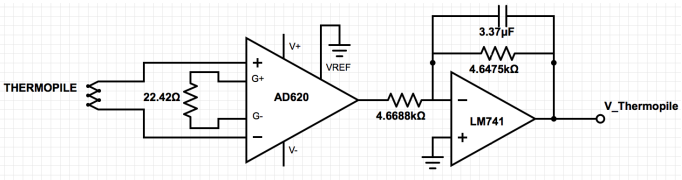

Figure . Circuit Diagram for the thermopile circuit

The thermistor's resistance changes with ambient temperature. A voltage divider circuit was used in order to calculate the resistance of the thermistor from measuring the voltage across and current through it. A voltage follower was used to isolate the voltage divider from the following signal conditioning. Since the voltage from the thermistor was nearly constant, we designed a filter with cutoff frequency of $0.5Hz$ and gain of 1 to remove high frequency noise in the signal.

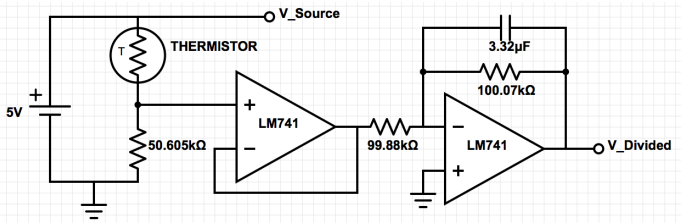

Figure . Circuit Diagram for the thermistor circuit

For the rangefinder, a $5V$ DC signal was applied across a 30.8Ω resistor in series with an IR LED ($940nm$) as an IR light source. The adjacent $940nm$ phototransistor then collected the IR light reflected from the surface of the skin. The output of a phototransistor is a current that is proportional to the intensity of light it collects. We chose a resistance of $5.605k\Omega$ through trial and error to obtain a voltage that would not saturate when the distance between the tip of our sensor and the phototransistor was within $5.5cm$. A voltage follower

was used for the phototransistor voltage before acquisition by the DAQ board prevent current from the phototransistor being diverted.

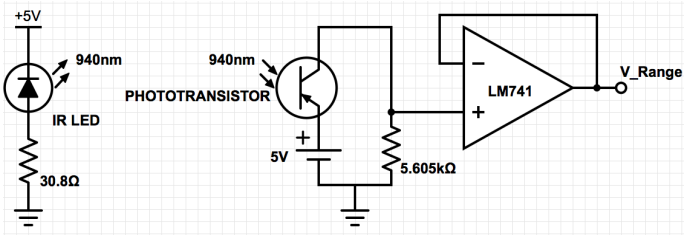

Figure . Circuit Diagram for the range finder

C. LabVIEW VI

1) Determination of Calibration Constants: Our LabVIEW VI acquired four signals from the DAQ board: Voltage from the thermopile ($V_{Thermopile}$), Voltage from the power supply (V_2), Voltage from the Thermistor ($V_{Thermistor}$), and voltage from the photodetector (V_{Range}). The first task of our LabVIEW VI was to calculate the resistance of the thermistor ($R_{thermistor}$), which we needed to calculate the ambient temperature (T_a). We used equation 1 to calculate $R_{thermistor}$. Then, using equation 2 we determined T_a of the thermistor.

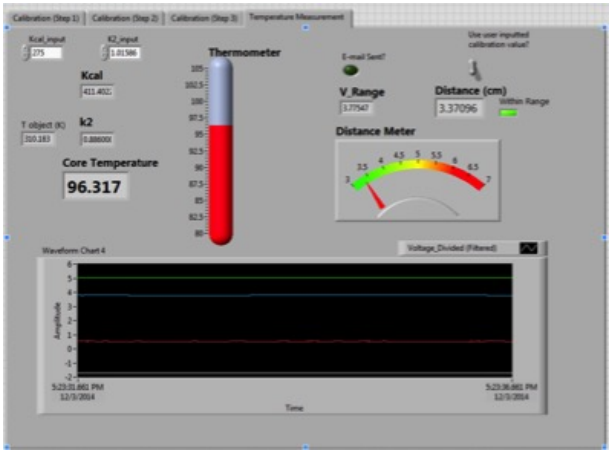

Figure . Front Panel for our temperature monitoring VI

To calibrate the IR thermometer we used a tab system on our LabVIEW VI. Three tabs were designated as calibration steps to determine the calibration constants needed to relate skin temperature at a particular location on the body to core body temperature. In the first step of calibration, T_obj (at the ear) was determined using an IR temperature gun and entered into the VI. The output of the first step was K_{cal}, which related $V_{thermopile}$ to T_{obj} and T_a, see equation 3. The second step of calibration used the result from step 1, k_{cal}, as an input to calculate T_{obj}. Then, the calibration constant, k_1, could be calculated by substituting equation 5 into equation 4. Next, we used k_1 to calculate core body temperature (T_c). Tc could be calculated using equation 6 which related the core body temperature to the ear temperature(T_e) and ambient temperature(T_a). In step 3 of calibration, knowing T_c we were able to solve for K_2, using equation 7, which related T_c, T_p, and T_a. The fourth tab in the LabVIEW VI was used to measure core body temperature from various positions on the body, using the constants calibrated in the first three steps. Therefore we used equation 7 with a calibrated K_2 value to solve for core temperature. We found that K_2 could be used to relate many different areas on the body to core temperature, not just the palm.

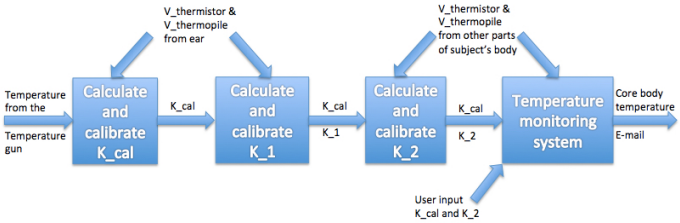

Figure . Flow Chart for Our LabVIEW procedures

2) Rangefinder: The VI used the inputted photodetector voltage to calculate distance of the object from the sensor using the inverse of the best fit line determined experimentally. The determination of the best fit line is detailed in the Results section below.

3) Email: Finally, the calculated core body temperature was analyzed to determine the person was at risk for hyperthermia or hypothermia. If the core body temperature was above $103°F$, the LabVIEW VI sent a warning email to a specified address to alert of potential fever or heat stroke and steps to lower body temperature. Similarly, if the core body temperature was below $95°F$, the VI sent a warning email to alert of hypothermia.

III. Results

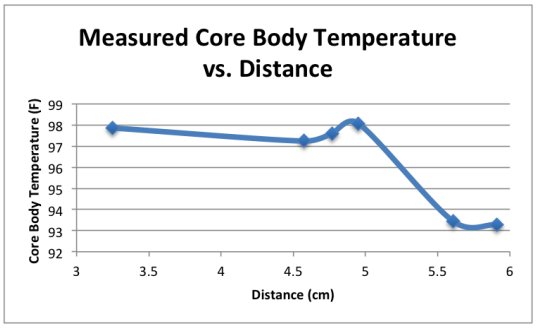

Figure . Graph for the Core Body Temperature vs. Distance

The rangefinder was calibrated by measuring the output voltage from the photodetector at various distances and performing regression to find a best-fit curve (Fig X). Three different fits were examined: linear ($R^2 = 0.84$), quadratic ($R^2 = 0.85$), and exponential ($R^2 = 0.87$). Although a quadratic fit was expected due to the $1/D^2$ profile of light intensity, an exponential fit was chosen due to a higher R^2 and simpler inverse solution when calculating distance from voltage.

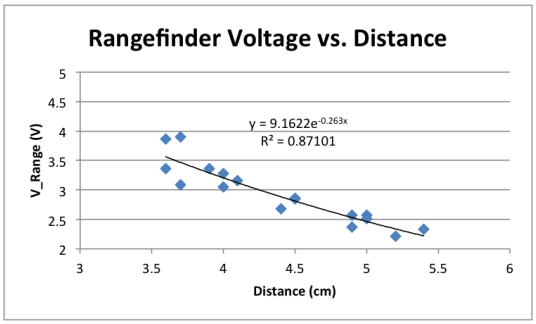

Figure . Graph for the Range Finder's Voltage vs. Distance

Following calibration, the accuracy of the rangefinder was validated by comparing the calculated distance with actual distance measured with a ruler (Table Y), for which a two-tailed T-test failed to find a statistical difference ($p = 0.797$). Core body temperature calculated from the palm was then measured as a function of distance (Fig Z). At a distance of 5cm away from the sensor, measured core body temperature was found to decrease. Thus, 5cm was chosen as the cutoff value in the LabVIEW VI as the maximum range of the sensor.

Rangefinder Distance	Actual Distance	% Error
3.4	3.5	2.86
4.41	4	10.25
4.76	4.5	5.78
5.08	5	1.6
5.52	5.5	0.36

Table . Comparison between measurement and rangefinder result

In the first day of recording results, we completed step one of calibration, measuring K_{cal} as a function of T_{ear}. Kcal was averaged for many participants and an average k1 constant that related T_{ear} to T_{core} was found (Table xx). To validate this k_1 constant, we measured T_{core} for each person using our system and compared to measured T_{core} values obtained using a commercial ear thermometer. A significant difference was not found ($p = 0.09$, paired t-test). This means that both our system and the commercial system gave similar readings for T_{core} when reading temperature at the ear.

K_{cal}	$1086.84 \pm 241.61 V/K^4$
k_1	1.293 ± 0.079

Table . Average Calibration Constant Values

The next lab session, we found that the calibration constants found from the previous day were no longer valid, necessitating we redetermine average values of K_{cal}, and k_1. These values were used to determine k_{2-palm}, a constant relating palm temperature to core body temperature via arterial heat balance. Once again, we compared T_{core} readings at the palm to T_{core} obtained using the commercial thermometer. We found a significant difference ($p = 0.009$) in these two readings, so we decided to determine k_2 values at the back of hand and neck instead to investigate whether more consistent readings would be yielded across test subjects. A statistically significant difference ($p = 0.03$) was found between T_{core} measured at the back of palm and T_{core} measured using the commercial thermometer. However, no statistical difference was found ($p = 0.36$) between T_{core} measured at the neck and by the commercial thermometer. Thus more accurate measures of T_{core} were taken at the ear or and the neck over the palm or the back of the hand. A table summarizing averaged final K_{cal}, k_1, and k_{2-neck} values are shown in (Table XX) below.

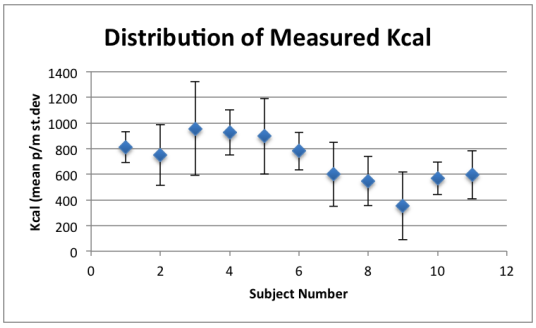

Figure . Graph for the variance of K_{cal} between different subject

K_{cal}	$681.94 \pm 317.05 V/K^4$
k_1	1.212 ± 0.084
k_2 palm	1.330 ± 0.543
k_2 back of hand	2.408 ± 0.662
k_2 neck	1.759 ± 0.777

Table . Average Calibration Constant Values for different parts of body

IV. Discussion and Conclusions

The experiment consisted of designing a radiation thermometry system using a thermopile that is sensitive to radiation given off as heat. Output voltage signals were filtered and amplified using conditioning circuits and acquired into LabVIEW. The LabVIEW VI allows for calibration of the device to determine core body temperature via temperature readings at the various locations on the body.

One reason that the palm may have worked poorly for determining core body temperature was due to large variance in temperature of subjects hands. Furthermore, hand temperatures may have changed over the course of the calibration step if the subjects hands cooled after having been in pockets or in contact with other parts of the body. Many variables also factor into palm temperature, such as blood flow, heat loss, and sweating, which result in large variation among the palm temperatures of different people. Because of this, it is difficult to determine a single constant that relates palm temperature to core body temperature for an entire population. At the neck, since a greater volume of blood close to the skin flows through, its temperature exhibited more consistency, beneficial for determining core body temperature.

A major source of variability was the sensitivity of the thermopile sensor. When determining the different calibration constants needed to calculate core body temperature from the voltages outputted from the sensor, there was considerable variation of calibration constants from person to person, as well as trial to trial. The connections between the sensor and wires connecting it to the breadboard were extremely sensitive and would output drastically different readings if the wires were disturbed even the slightest amount. One way to fix this would be to design a case for the sensor and package the

separate wires into a single wire. Additionally, values of K_{cal} in the first step of calibration varied tremendously because it was calculated by taking the fourth power of T_{obj} and T_a. Thus, small changes in T_{obj} or T_a from trial to trial were magnified greatly and affected the calculation of K_{cal}, which affected the calculation of all subsequent calibration constants.

For our range finder, one problem was the difference in skin reflection index for different subjects.To solve the problem, we measured calibrated the device to many different people and performed an exponential fit to the data. The problem with this was that it would not be an accurate distance for that specific person. However, the purpose of the range finder was to verify that the distance between the sensor and the target was well-within an acceptable range, so not being able to give an accurate distance should be acceptable.

There is a possibility that the temperature gun or the ear thermometer is not accurate. Since we do not have more thermometers to validate their accuracy, we cannot be certain. For our experiments, we assumed that the temperature from both of them are accurate and we calibrated our device to their values.

Another notable fact was that the ear thermometer that we bought took 512 samples of measurements and reported the highest one, according to its specification. In this way it would eliminate the problem of false positiveS (the patient is having a high temperature but the thermometer failed to report it). For an at-home thermometer that would only be used when one may have a fever, it is appropriate. However, for a temperature monitoring system, this would be a bad idea. We averaged the measured voltage for one second, and then performed the calculations. In this way, we eliminated some of the noise and avoided some of the inaccuracy caused by accidental fluctuation in our sensor. Yet, since it is a different method compared with the one that is used in the ear thermometer, there would be some difference between the two temperature readings.

Finally, the use of a packed thermopile and thermistor was a limitation for our thermometer design. The thermistor resistance was prone to increasing as the device was held and heated, increasing values of $T_{ambient}$. During our experiment, we found that after testing it for a long time, values (such as K_{cal} and distance) changed compared with our initial measurements. Since the voltage outputted from the thermopile was related to both the object temperature and thermopile temperature, if the thermopile temperature changed, the output result would have been influenced.

V. Application

To improve this system, we could purchase a higher quality thermopile sensor. Our device had extremely sensitive connections and did not respond well to any movement of our system. A higher quality sensor would allow us to create a more compact and portable device, which may improve the accuracy of our results drastically. This improvement may allow us to determine average calibration constants that can be used over a large population. This would save a lot of time because each person would not have to calibrate the device to their own body before use, rather they could use predetermined constants. Also we may design a structure to fix the sensor in place, and use wires that are pre-packed (a single wire with several coils inside) to decrease the influence of wires being not stable and leading to noise. We didnt consider about how to fix the sensor onto a specific location on the patient, which may be a further step that can be done.

With a thermopile sensor with higher-quality, we then may be able to collect data from more subjects. In this way, we would be able to determine k_{cal}, k_1, and k_2 values that are applicable to a much wider group of subjects, and giving them a better results despite individual variance..

Acknowledgment

The authors would like to thank the Biomedical Engineering Department at the University of Michigan for funding this project, as well as Professor Dennis Claflin, and graduate student Patrick Ingram for help with this project.

References

[1] Pompei, F., Ambient and perfusion normalized temperature detector, U.S. Patent 6 299 347, Oct. 9, 2001.

Appendix A
Equations

$$R_{Thermistor} = (V_{source} - V_{Divided}) \cdot \frac{R_2}{V_{Divided}} \quad (1)$$

$$\frac{1}{T_{Thermistor}} = \frac{1}{T_a} = \frac{1}{T_0} + \frac{1}{B} \cdot ln(\frac{R_{Thermistor}}{R_0}) \quad (2)$$

$$V_{Thermopile} = K_{Cal}(T_{obj}^4 - T_a^4) \quad (3)$$

$$K_1 = 1 + \frac{h}{pc}[1] \quad (4)$$

$$\frac{h}{pc} = 0.00108T_{obj}^2 - 0.2318T_{obj} + 12.454[1] \quad (5)$$

$$T_c = K_1(T_e - T_a) + T_a \quad (6)$$

$$T_c = K_2(T_p - T_a) + T_a \quad (7)$$

$$V_{range} = \alpha e^{-\beta D} \quad (8)$$

Equation 1 comes from the voltage divider circuit where the thermistor is in series with resistor R_2.

Equation 2 is the characteristic equation of the thermistor that we used. According to the spec. sheet, we have R_2 to be $50,605\Omega$, T_0 was $298K$, and B was $3964K$.

Equation 3 is established because the power of IR radiation given by an object is related to the fourth power of its temperature, and we assumed that the voltage given by the thermopile is proportionally related to the power of the IR radiation that it detects.

For equation 4, we have the following constants as specified: h is the heat transfer coefficient, p is the blood perfusion rate per unit area of skin, and c is the specific heat of blood. Equation 5 is a relationship that we found from literature.

Equation 6 is to relate the ear temperature to core body temperature, and 7 is to relate part of our body's temperature to core body temperature.

APPENDIX B
BODE PLOT

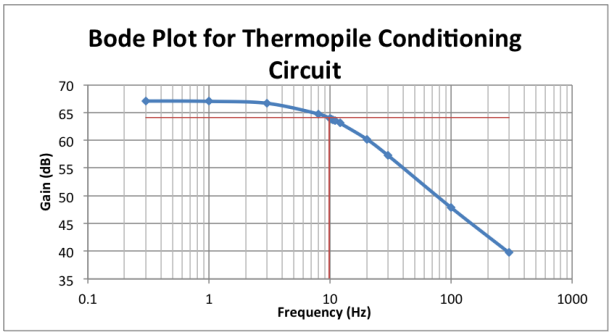

Figure . Bode Plot for the thermopile circuit

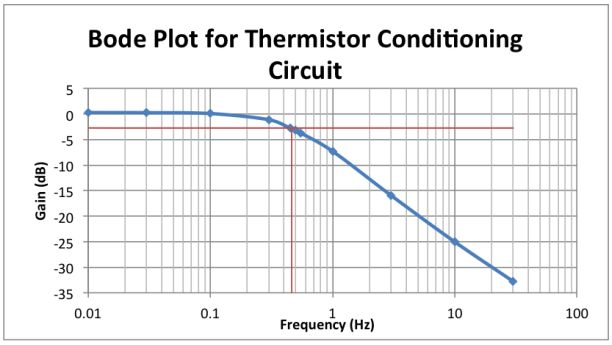

Figure . Bode Plot for the thermistor circuit

APPENDIX C
LABVIEW

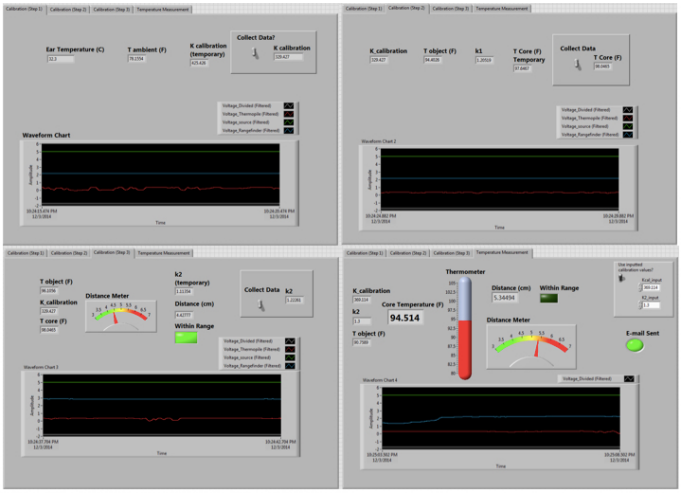

Figure . Front panel for all the tabs of our LabVIEW VI